Geological Survey of Canada
Open File 8386

TOMODENSITOMETRY APPLIED TO CHARACTERIZE ROCK PROPERTIES OF A CONVENTIONAL HETEROGENEOUS CARBONATE RESERVOIR IN QUEBEC

S. Larmagnat[1], P. Francus[2], M. Des Roches[2], L.-F. Daigle[2], J. Raymond[2], M. Malo[2], and A. Aubiès-Trouilh[3]

Introduction

As part of a new Industry-Academy research partnership, this project intended to assess the reservoir potential of lower Silurian carbonates (Sayabec Formation) within a prospective play (Massé Structure) in the lower St-Lawrence river area. Carbonate reservoirs are known to be genetically complex and spatially heterogenous (bioclasts, fractures) and their diagenetic history is responsible for either creation or occlusion of porosity. Tomodensitometry has been commonly applied to core analyses within the Oil and Gas sector in order to analyse porosity, fractures patterns, or assess fluid flow in porous rocks (Akin and Kovscek, 2013; Taud et al., 2005; Geiger et al., 2009). However, the methodology is mainly applied to clastic reservoir rocks or relatively homogenous carbonate reservoir (Baniak et al., 2013; Van Geet at al., 2003). In the Massé structure, the Sayabec Formation displays a wide range of heterogenous carbonate facies interbedded with siltstones (Fig. 1; Tab. 1). The natural heterogeneity of facies translate into a large range of porosity type and values. Industry partner needs a rapid and efficient tool to optimize their drilled wells in order to locate the most porous and permeable intervals and help planning future wells.

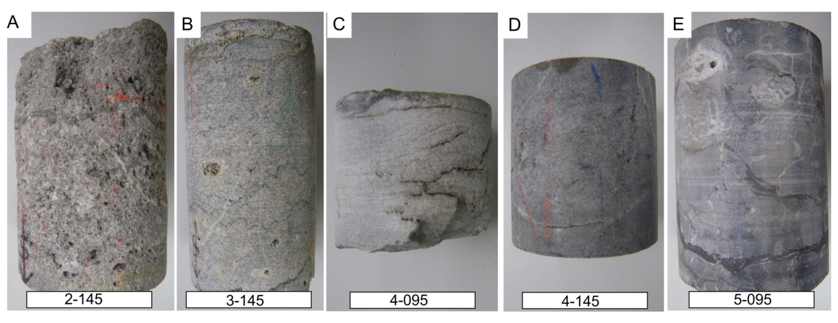

Figure 1: Photograph of the five whole core samples used for this study. These samples belong to the Sayabec Formation in Massé No. 1 well drilled within the Massé structure. Core samples are 4,5 cm in diameter and their length ranges from 40 to 85 mm.

Sample #	Lithology and grain size	Comments
2-145	Coarse-grained sandstone, with good to moderate sorting	Pluri-millimetric open spaces at the surface and argillaceous
3-145	Fine-grained limestone, with good sorting	Macropores visible at the surface (moldic porosity) and stylolithes
4-095	Fine-grained argillaceous limestone, with good sorting	Several thin fractures visibles at the surface and only partially colmated
4-145	Fine to medium-grained, sandy limestone (or calcareous sandstone), with good sorting	Obliques and pseudo-horizontal thin fractures partially colmated
5-095	Fine-grained, bioclastic limestone, with bioturbation and macroscopic bioclastic fragments	Rare pores visibles at the surface, including partially dissoved bioclasts. Thin, irregular, argillaceous seams

Table 1: Detailed visual description of the five core samples including lithology, grain size and main sedimentary features.

Methodology

CT measurements were performed using a Siemens SOMATOM Definition AS+ 128 at INRS-ETE. Images were recorded in DICOM format and visualization was made with Fiji software. A 40 m long section was scanned. Five isolated samples were additionally scanned in a dry state and then flooded with water (Fig. 2;Tab. 2). Core flooding was conducted at room temperature using an in-house core flooding system (Fig. 2). The method involves scanning of the core samples under vacuum and then at different times when it is progressively saturated with water. An image substraction of final and initial stage (saturated and dry) was performed using Matlab software allowing a visualization of macropores network and calculation of porosity (Fig. 3).

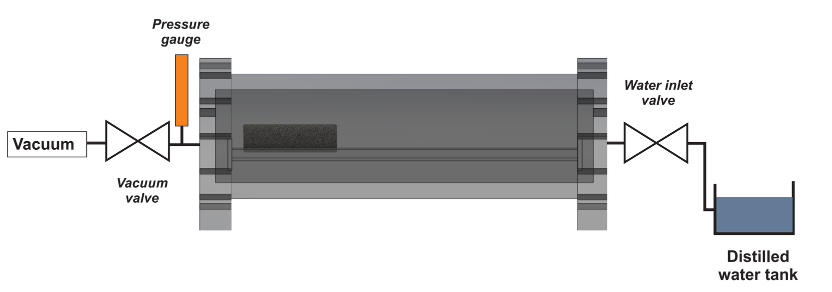

Figure 2: Schematic representation of the core flooding experiment run under CT scanner. The main parts of the flooding apparatus are a 50 cm long PVC tube, a pumping system and a pressure gauge. Core flooding was performed under vacuum using distilled water.

$$\%_{matrix} + \%_{porosity} = 1$$
$$D_{dry} = D_{matrix}.\%_{matrix} + D_{gaz}.\%_{pores}$$
$$D_{saturated} = D_{matrix}.\%_{matrix} + D_{liquide}.\%_{pores}$$

$$\%_{pores} = \frac{D_{dry} - D_{saturated}}{D_{gas} - D_{liquide}}$$

Figure 3: The porosity was calculated using the equation above. Since only pore density will change, grains density and composition are not needed (Boespflug et al., 1994). Fluid densities are known as part of CT calibration ($D_{gas} = D_{air} = -1000$ HU; $D_{liquid} = D_{water} = 0$ HU).

Density changes associated with the infiltration of water could be low when porosity is low. In such cases, image noise is problematic and could outweigh the density variation associated with the water saturation. Pini and Madonna (2016) approach was adopted and examined how the level of noise changes when averaging several scans or decreasing the resolution, and how this ultimately affects the porosity calculation (Fig. 4; 5). The number of scan to average was then set to three in order to the get the shortest acquisition time with the lowest image noise.

Parameter	40 m cored interval (bi-energy)	Isolated core samples
Acquisition parameters		
kVp	120/140	140
mAs	1255/1057	700
Pitch	0.35	0.3
Collimation	40 x 0.6 mm	16 x 0.6 mm
Reconstruction parameters		
Filter	J70h/3	U70u
F.O.V	50 mm	60 mm
Pixels spacing	0.0977 mm	0.117 mm
Thickness	0.6 mm	0.6 mm
HU scaling	Normal and extented	Normal

Table 2: Summary of CT-scanner parameters values for both acquisition and reconstitution stages.

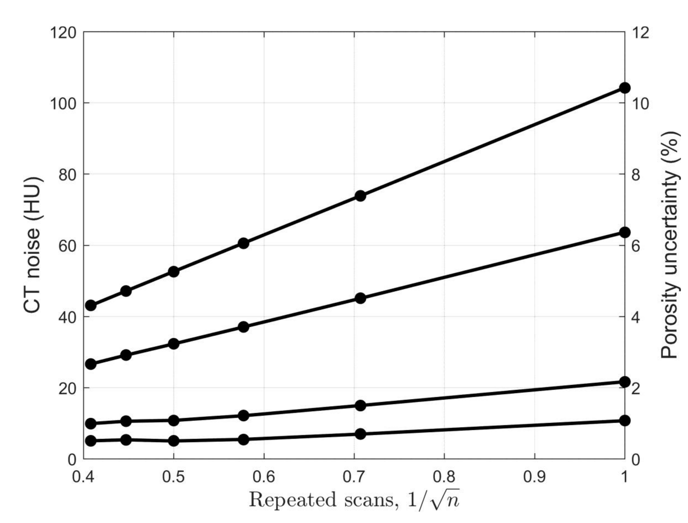

Figure 4: Impact of noise level on porosity calculation and its uncertainty level (adopted from Pini and Madonna, 2016).

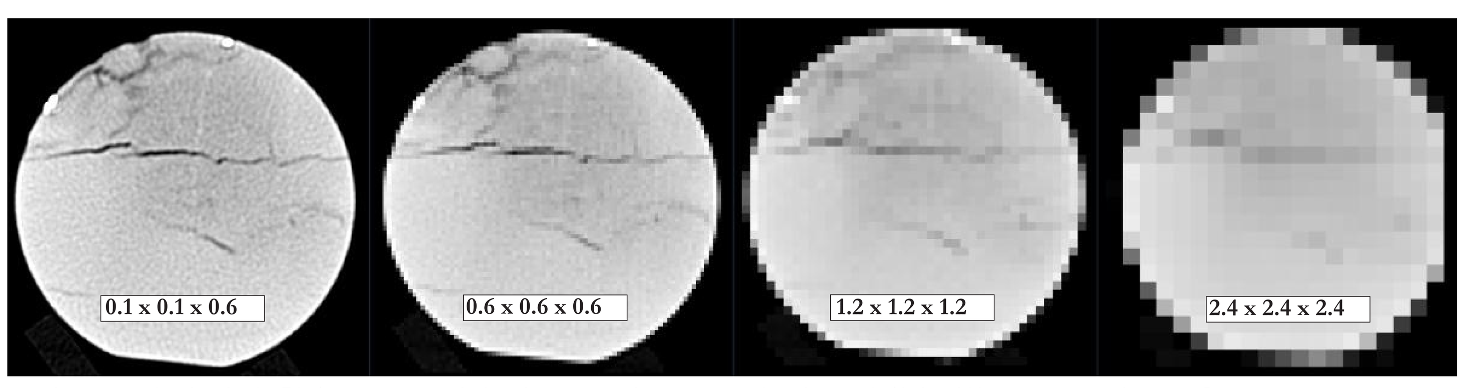

Figure 5: Axial CT-scans with decreasing resolution. This illustrates how fine structures (such as fracture) could remain undetected if the resolution is too low. The spatial resolution was then set to 0.1 x 0.1 x 0.6 mm.

Results

Macropores distribution, size and architecture

X-ray tomography images showed good contrast between pores, grains/matrix and dense mineral phases (Fig. 6B-D). This allowed us to generate 3D images of the macropores network documenting their geometry, connectivity and distribution (Fig. 7). The method delivers informations about the porosity within a sample that cannot be obtained with conventional gas porosimeter analyses.

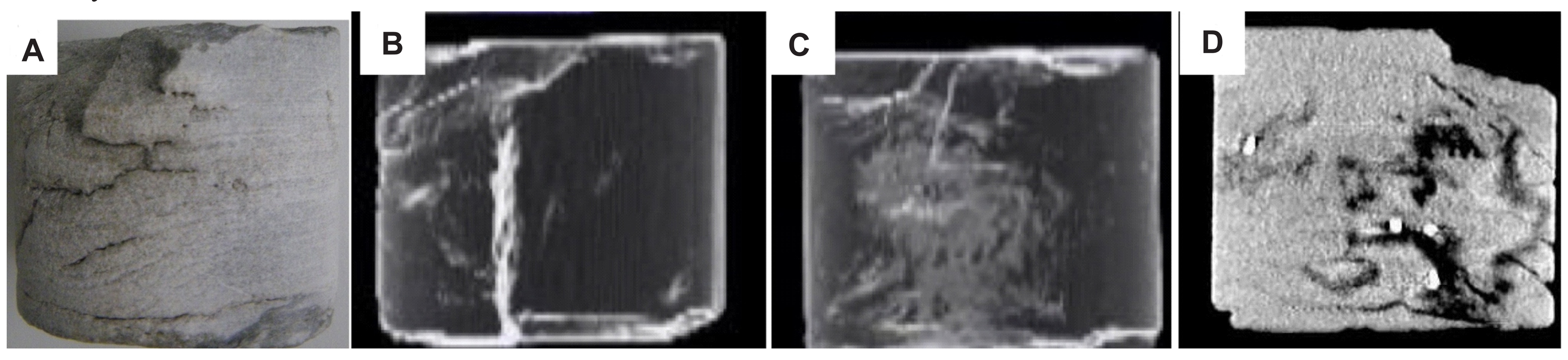

Figure 6: Photograph (A) and CT-scan images (B-D) obtained for sample 4-095. CT images include: coronal (B) and sagittal (C) CT image with MinIP (minimum intensity) projection and coronal intensity image (D). In the later, black areas correspond to open spaces whereas white areas correspond to the densest materials (possibly pyrite).

Density(porosity) trend along depth

By applying statistical parameters to CT-scan dataset, tomodensitometry can provide rapid information about sample heterogeneity and density (porosity) variation along depth (Fig. 8). These vertical trends could easily be compiled with conventional wireline log data.

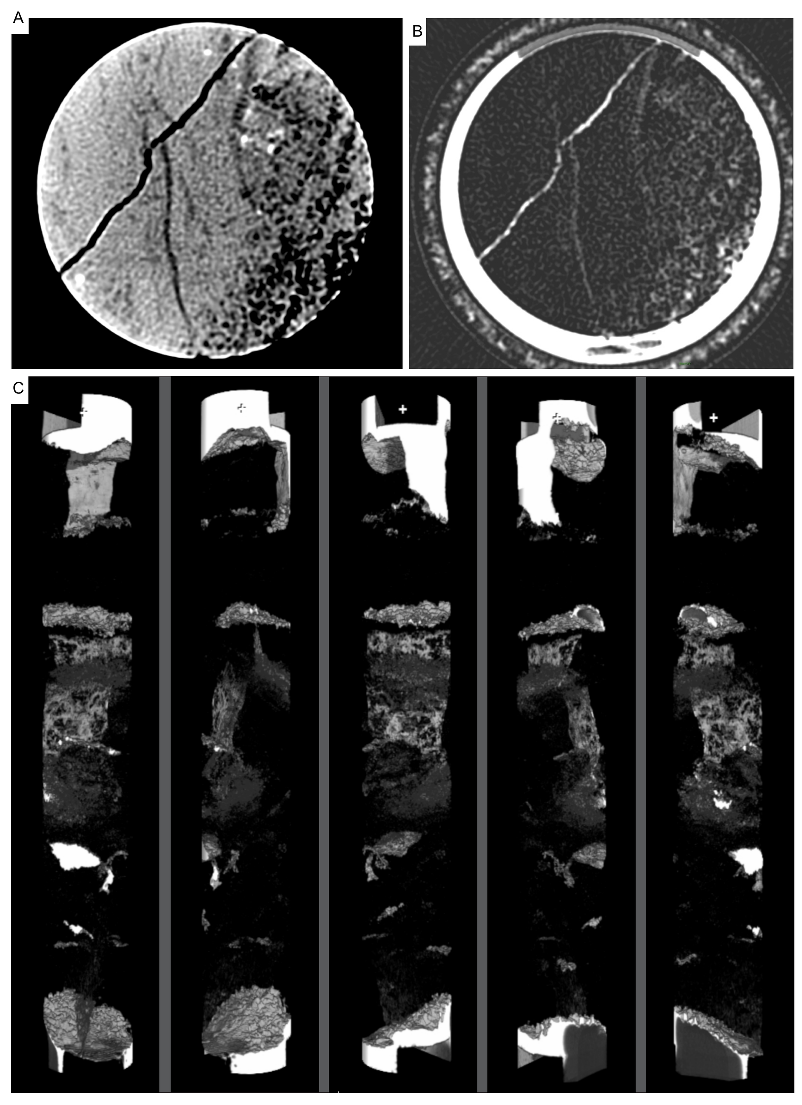

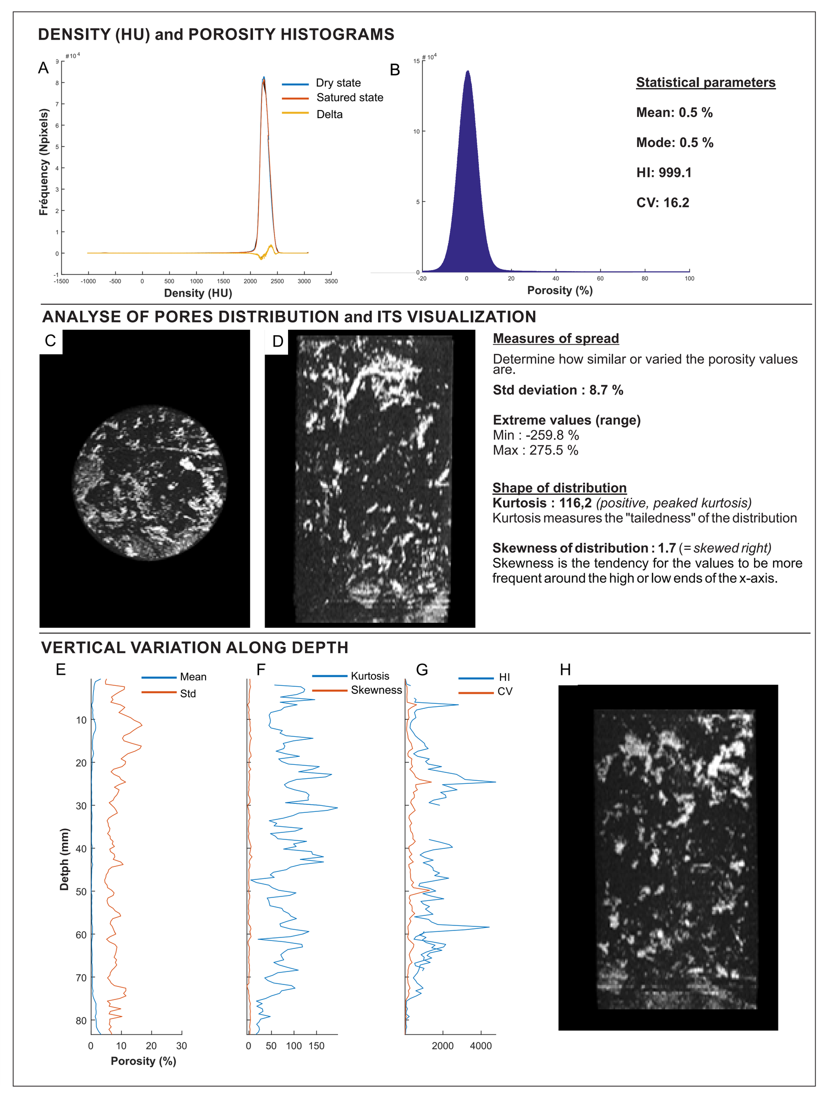

Figure 7: Macropores geometry within highly porous dolomitized sample. (A) Axial CT-scan compared to (B) axial section through the porosity matrix. (C) Five MinIP (minimum intensity projections) at 70 degrees intervals (porosity matrix).

Figure 8: Compilation of CT-scan results for sample 3-145. HI (heterogeneity index) and CV (coefficient of variation) parameters are adopted from Caliskan and Shebatalhamd (2015).

Role of microporosity

The mathematical comparison of the two density matrices (saturated and dry) documents the ease to partially or totally saturate samples. In few cases, the filling of pore spaces is documented whereas macropores were not macroscopically connected (Fig. 9). This reveals the role played by microporosity in connecting the macropores and allowing the water to flow through. Furthermore, an alternative way to estimate porosity using CT-scan data is to apply thresholding techniques (Taud et al., 2005). By segmenting the macropores, the method gives rapidly a minimal porosity value of the specimen.

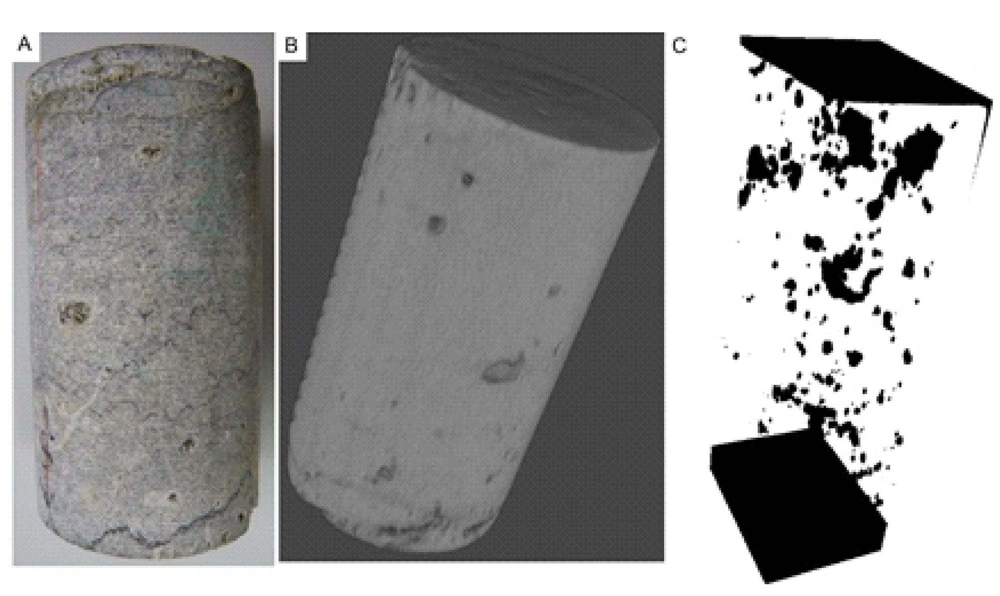

Figure 9: (A) Photograph of the core sample 3-145, a fine-grained, well sorted limestone. Open pores and thin pseudo-horizontal stylolithes (underlined by opaque minerals) are visible at the surface. (B) 3D CT image of the sample. (C) 3D MinIP projection. The porosity calculation performed on density matrices gave a value of 1.75% of the total sample volume. In comparison, helium gas porosimeter gave a value of 1.3% for the same sample which would correspond to a porosity underestimation made by the helium porosimeter of approximately 35%.

Conclusions and future works

Tomodensitometry is a valuable tool for qualitative and quantitative characterization of heterogeneous carbonate reservoir facies in 3D. It provides a large set of 3D data regarding the porosity such as macropores dimensions and geometry, or macropores distribution. With a simple coreflooding system, the comparison between a dry and saturated states can revealed the role played by microporosity. Future works intend to optimize the coreflooding system to perform multiple core sections simultaneously. Another important step forward is the calibration of the method using standard rock samples commonly used in the Oil and Gas sector, such as the Indiana Limestone or the Berea Sandstone.

References

Akin, S. and A. Kovscek (2003). "Computed tomography in petroleum engineering research." Geological Society, London, Special Publications 215(1): 23-38.
Baniak, G. M, M. K. Gingras and S. G. Pemberton (2013). "Reservoir characterization of burrow-associated dolomites in the Upper Devonian Wabamun Group, Pine Creek gas field, central Alberta, Canada." Marine and Petroleum Geology 48: 275-292.
Boespflug, X., N. Ross , B. Long and J. Dumais (1994). "Tomodensitométrie axiale: relation entre l'intensité tomographique et la densité de la matière." Canadian Journal of Earth Sciences 31(2): 426-434.
Caliskan, S. and A. Shebatalhamd (2015). Statistical interpretation of heterogeneity based on the CT scanning data. 2nd International Conference on Tomography of Materials and Structure (ICTMS). Quebec. Abstract book
Geiger, J., Z. Hunyadfalvi and P. Bogner (2009). "Analysis of small-scale heterogeneity in clastic rocks by using computerized X-ray tomography (CT)." Engineering Geology 103(3): 112-118.
Pini, R. and C. Madonna (2016). "Moving across scales: a quantitative assessment of X-ray CT to measure the porosity of rocks." Journal of Porous Materials 23(2): 325-338.
Taud, H., R. Martinez-Angeles, J. F. Parrot and L. Hernandez-Escobedo (2005). "Porosity estimation method by X-ray computed tomography." Journal of Petroleum Science and Engineering 47(3–4): 209-217.
Van Geet, M. and R. Swennen (2001). Quantitative 3D-fracture analysis by means of microfocus X-Ray Computer Tomography (μCT): An example from coal. Geophysical Research Letters, 28(17), 3333-3336.

[1]Geological Survey of Canada, 490, rue de la Couronne, Québec, Quebec, G1K 9A9
[2]INRS, Centre Eau Terre Environnement, 490, rue de la Couronne, Québec, Quebec G1K 9A9
[3]Ressources & Énergie SQUATEX Inc., 7055, boul. Taschereau, bureau 500, Brossard, Quebec J4Z 1A7

For more information contact S. Larmagnat (stephanie.larmagnat@canada.ca)

Permanent link: https://doi.org/10.4095/308112

This publication is available for free download through GEOSCAN (http://geoscan.nrcan.gc.ca/).

OPEN FILE
DOSSIER PUBLIC
8386
GEOLOGICAL SURVEY OF CANADA
COMMISSION GÉOLOGIQUE DU CANADA
2018

Publications in this series have not been edited; they are released as submitted by the author.
Les publications de cette série ne sont pas révisées; elles sont publiées telles que soumises par l'auteur.

Recommended citation
Larmagnat, S., Francus, P., Des Roches, M., Daigle, L.-F., Raymond, J., Malo, M., and Aubiès-Trouilh, A., 2018. Tomodensitometry applied to characterize rock properties of a conventional heterogeneous carbonate reservoir in Quebec; Geological Survey of Canada, Open File 8386, 1 poster. https://doi.org/10.4095/308112

Natural Resources Canada
Ressources naturelles Canada